(2+1)-dimensional noncommutative CP^{N-1} model

E. A. Asano,* M. Gomes,† A. G. Rodrigues,‡ and A. J. da Silva§
Instituto de Física, Universidade de São Paulo, Caixa Postal 66318, 05315-970, São Paulo–SP, Brazil
(Received 21 July 2003; published 22 March 2004)

We investigate possible extensions of the $(2+1)$-dimensional CP^{N-1} model to noncommutative space. Up to the leading nontrivial order of $1/N$, we prove that the model restricted to the left fundamental representation of the gauge group is renormalizable and does not have dangerous infrared divergences. In contrast, if the basic field φ transforms in accord with the adjoint representation, infrared singularities are present in the two-point function of the auxiliary gauge field and also in the leading correction to the self-energy of the φ field. These infrared divergences may produce nonintegrable singularities leading at higher orders to a breakdown of the $1/N$ expansion. Gauge invariance of the renormalization procedure is also discussed.

DOI: 10.1103/PhysRevD.69.065012 PACS number(s): 11.10.Nx, 11.10.Gh, 11.10.Lm, 11.15.−q

I. INTRODUCTION

One of the main characteristics of field theories defined in noncommutative space is the infrared-ultraviolet (IR-UV) mixing, which, even in models without massless particles, leads to the appearance of infrared divergences and, as a consequence, to the breakdown of the perturbative scheme in many renormalizable models (see Ref. [1] for recent reviews).

The presence of infrared divergences in ordinary field theory signals that one may be expanding around a point of nonanalyticity of the exact solution. It may indicate the existence of nonperturbative effects that cannot be reached by a power series expansion on the perturbative coupling. In such a case, two possible approaches are envisaged. One may try resummation to rearrange the perturbative series to get a better behaved expansion. A difficulty in this method is the identification of a parameter to control different orders of the new series. Another possible procedure is to enlarge the theory with new interactions, which, hopefully, will cancel the IR divergences leading to a new expansion without the singularities mentioned. For noncommutative theories both methods have been considered in the literature [2–8]. In fact, it has been argued that resummation may be efficiently controlled by the Wilsonian renormalization group, in the manner of Polchinski [9]. On the other hand, it has been shown that there exists a special class of theories, namely supersymmetric models, which are natural candidates to be consistent in noncommutative space, at least as far as renormalization is concerned. This has been proven to be correct for the noncommutative versions of the four-dimensional Wess-Zumino model [4,5] and the three-dimensional nonlinear sigma model [6] to all orders and also, at least up to one-loop order, for some supersymmetric gauge models [7,8]. However, noncommutative theories are so subtle and unusual that detailed investigations even in nonsupersymmetric theories are still in order.

Proceeding with the aforementioned investigations here we will study the noncommutative CP^{N-1} model. In this model local gauge invariance is attained through a composite field that, at least classically, is not dynamical. This simplifying aspect makes the model a good candidate for the investigation of general properties of gauge fields in noncommutative space. The introduction of a gauge symmetry in noncommutative space produces a very rich structure in the sense that, even for the $U(1)$ gauge group, there are three alternative ways in which the basic matter field could transform.

We begin our study by considering here the pure CP^{N-1} model, i.e., without fermionic matter fields. As it happens with its real $O(N)$ symmetric counterpart, the nonlinear sigma model is perturbatively renormalizable only in two-dimensions for the commutative version of the model. However, it is $1/N$ expandable in both two and three space-time dimensions [10,11]. Dynamical generation of gauge degrees of freedom and confinement are interesting aspects of the $1/N$-expansion of the two-dimensional model [10]. When coupled to fermions either minimally or in a supersymmetric fashion the quanta of the basic field φ are liberated and exact S matrices are found [12].

The three-dimensional model also possesses some interesting properties. Its $1/N$ expansion presents phases in which the basic fields are either massive or massless [11]. In particular, if a Chern-Simons term is added [13–15] one finds radiative corrections to the topological mass at the next-to-leading order of $1/N$ [13]. In this study we will work in the unbroken phase (massive φ) of the $(2+1)$-dimensional model.

In the noncommutative CP^{N-1} model, because of the underlying noncommutativity, we may consider the basic field as belonging alternatively to a fundamental (left or right) or to the adjoint representation of the gauge group. We present a detailed discussion of the renormalization of the model in the fundamental representation up to the next-to-leading order of $1/N$. The model turns out to be renormalizable but the existence of planar and nonplanar graphs with distinct UV behaviors unveils some interesting features. In particular, some graphs in the commutative case, as a consequence of charge conjugation, do not contribute. However, these graphs

*Electronic address: asano@fma.if.usp.br
†Electronic address: mgomes@fma.if.usp.br
‡Electronic address: alexgr@fma.if.usp.br
§Electronic address: ajsilva@fma.if.usp.br

in the noncommutative setting where charge conjugation no longer holds [16], produce non-null results. Despite this, at least up to the leading nontrivial order of $1/N$, the model turns out to be renormalizable and free of dangerous infrared divergences [17].

In contradistinction to the left fundamental representation, the adjoint representation, already at leading order, presents infrared singularities. The implications of these singularities are twofold. On one hand, the divergences that occur in the gauge sector suggest the existence of strong long-range forces. In addition, in the φ field self-energy corrections there are also quadratic infrared divergences, which at higher order will destroy the $1/N$ expansion. It could be argued that, similarly to noncommutative QED_4 [18], this behavior may be ameliorated by the inclusion of fermionic fields. This will be the subject of a subsequent paper where we will discuss the dynamical generation of a Chern-Simons term. The elimination of the (dangerous) IR-UV mixing in a supersymmetric extension of the model will be also investigated.

This work is organized as follows. In Sec. II the possible representations for the noncommutative CP^{N-1} model are presented. In Sec. III we investigate the leading contributions to the case in which the basic field belongs to the left fundamental representation and examine in detail both the UV and IR divergences up to the next-to-leading order of $1/N$. Dimensional regularization is used and we prove that the model is free from dangerous divergences (i.e., nonrenormalizable or nonintegrable IR divergences are absent). In Sec. IV we analyze the behavior of the Green functions when the basic fields belong to the adjoint representation. In this situation we verify explicitly the presence of IR-UV mixing, which jeopardizes the consistency of the model. In Sec. V we present some concluding remarks. In the Appendix we discuss some additional properties of the model.

II. THE NONCOMMUTATIVE CP^{N-1} MODEL

The commutative CP^{N-1} model is specified by the Lagrangian density

$$\mathcal{L}=(D_\mu\varphi)^\dagger D^\mu\varphi-m^2\varphi^\dagger\varphi+\lambda\left(\varphi^\dagger\varphi-\frac{N}{g}\right), \tag{1}$$

where φ_i, $i=1,\ldots,N$, are complex scalar fields, $D_\mu\varphi\equiv(\partial_\mu+iA_\mu)\varphi$ is the covariant derivative of φ, and A_μ is an auxiliary gauge field [classically it is just a convenient notation for the composite field $(g/N)(\varphi^\dagger\overleftrightarrow{\partial_\mu}\varphi)$]; λ is the Lagrange multiplier field enforcing the constraint $\varphi^\dagger\varphi=N/g$. Because of this constraint, the presence of the mass term is classically not relevant. At the quantum level, m will be identified with the physical mass for the quanta of the φ field insofar as one enforces a zero vacuum expectation value for the λ field. The discussion of this fact is entirely analogous to the one in the $O(N)$ nonlinear sigma model and will not be pursued here [6]. The noncommutative versions of the model are obtained by replacing the ordinary pointwise product by the Moyal product [19,20], which is associative and satisfies [21]

$$\phi_1(x)*\phi_2(x)=\lim_{y\to x}e^{(i/2)\Theta^{\mu\nu}(\partial/\partial y^\mu)(\partial/\partial x^\nu)}\phi_1(y)\phi_2(x), \tag{2}$$

where the constant and antisymmetric matrix $\Theta_{\mu\nu}$ gives a measure of the noncommutativity strength. To avoid possible unitarity and/or causality problems [22] we will set $\Theta_{0i}=0$ (see also Ref. [23]).

As the Moyal-ordered product is noncommutative, we shall investigate three possible representations for the matter field.

(1) Left representation:

$$\varphi\to(e^{i\Lambda})_*{*}\varphi, \tag{3}$$

$$\varphi^\dagger\to\varphi^\dagger{*}(e^{-i\Lambda})_*, \tag{4}$$

where Λ is the gauge transformation function and

$$(e^{i\Lambda})_*\equiv 1+i\Lambda+\frac{i^2}{2}\Lambda{*}\Lambda+\cdots. \tag{5}$$

(2) Right representation:

$$\varphi\to\varphi{*}(e^{-i\Lambda})_*, \tag{6}$$

$$\varphi^\dagger\to(e^{i\Lambda})_*{*}\varphi^\dagger. \tag{7}$$

(3) Adjoint representation:

$$\varphi\to(e^{i\Lambda})_*{*}\varphi{*}(e^{-i\Lambda})_*, \tag{8}$$

$$\varphi^\dagger\to(e^{i\Lambda})_*{*}\varphi^\dagger{*}(e^{-i\Lambda})_*. \tag{9}$$

To keep the action unchanged under these transformations, the usual derivatives are replaced by covariant derivatives defined as

$$D_\mu\varphi=\partial_\mu\varphi+iA_\mu{*}\varphi, \quad \text{left representation,} \tag{10}$$

$$D_\mu\varphi=\partial_\mu\varphi-i\varphi{*}A_\mu, \quad \text{right representation,} \tag{11}$$

$$D_\mu\varphi=\partial_\mu\varphi+iA_\mu{*}\varphi-i\varphi{*}A_\mu, \quad \text{adjoint representation.} \tag{12}$$

In all three above representations, the gauge field transforms as

$$A_\mu\to(e^{i\Lambda})_*{*}A_\mu{*}(e^{-i\Lambda})_*+i[\partial_\mu(e^{i\Lambda})_*]{*}(e^{-i\Lambda})_*. \tag{13}$$

For sake of simplicity, we shall restrict our analysis to the left and adjoint representations, as the analysis for right and left representations are very similar. In the left representation the part of the Lagrangian containing the auxiliary field λ must be written either as

$$\lambda{*}\left(\varphi^\dagger{*}\varphi-\frac{N}{g}\right) \tag{14}$$

if λ does not change or

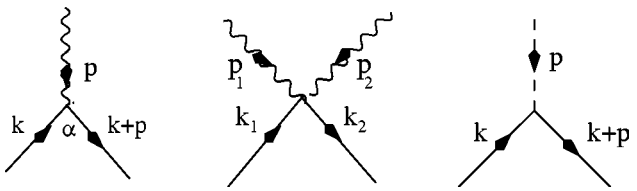

FIG. 1. Interaction vertices associated to the Lagrangian (17). The propagators for the A_μ, λ, and φ fields are represented by wavy, dashed, and continuous lines, respectively. For the complex field, charge flows in the opposite direction to the one indicated.

$$\lambda * \left(\varphi * \varphi^\dagger - \frac{N}{g} \right) \tag{15}$$

if λ changes according to the adjoint representation.

If φ belongs to the adjoint representation, then λ also belongs to this representation and the constraint part of the Lagrangian should be of the form

$$\lambda * \left(a \varphi^\dagger * \varphi + b \varphi * \varphi^\dagger - \frac{N}{g} \right), \tag{16}$$

where a and b are free parameters. In what follows, no matter what representation for the φ field is adopted, we always assume that λ belongs to the adjoint representation. As shall be clear in the next section, a great advantage of this assignment is the independence of the λ and A_μ fields in the fundamental representation (at the leading order of $1/N$). With this choice, the noncommutative action for the CP^{N-1} model in the left representation reads

$$\mathcal{L} = (D_\mu \varphi)^\dagger * D^\mu \varphi - m^2 \varphi^\dagger * \varphi + \lambda * \left(\varphi * \varphi^\dagger - \frac{N}{g} \right). \tag{17}$$

As we will do shortly, to complete this Lagrangian we shall add to it a gauge-fixing and Faddeev-Popov terms.

III. THE NONCOMMUTATIVE CP^{N-1} MODEL IN THE LEFT REPRESENTATION

For the left fundamental representation our graphical notation prescribes the following Feynman rules:

$$\Delta_\varphi(p) = \frac{i}{p^2 - m^2 + i0} \tag{18}$$

for the φ propagator and

$$iA^\alpha (\varphi \partial_\alpha \varphi^\dagger - \partial_\alpha \varphi \varphi^\dagger) \ \text{vertex} \ \leftrightarrow \ -i(2k+p)_\alpha e^{-ik \wedge p}, \tag{19}$$

$$A_\mu A_\nu \varphi \varphi^\dagger \ \text{vertex} \ \leftrightarrow \ 2ig_{\mu\nu} e^{-ik_1 \wedge k_2} \cos(p_1 \wedge p_2), \tag{20}$$

$$\lambda \varphi \varphi^\dagger \ \text{vertex} \ \leftrightarrow \ ie^{-ik \wedge p} \tag{21}$$

for the vertices (see Fig. 1), where $a \wedge b \equiv \frac{1}{2} a^\mu b^\nu \Theta_{\mu\nu}$. Except for some graphs containing the quadrilinear vertex (20), in the left representation, new features associated with the noncommutativity are present only for graphs with more than two vertices. This fact depends crucially on our choice of λ field as belonging to the adjoint representation, which fixes the sign of the phase in Eq. (21). In particular, the leading $1/N$ contribution for the mixed propagator $\langle T \lambda A_\mu \rangle$ is the same as in commutative situation and therefore vanishes, due to Lorentz covariance.

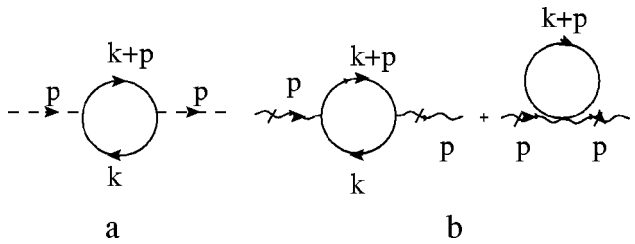

FIG. 2. Diagrams contributing to the proper functions of the λ and A_μ fields.

Contrary to the $O(N)$ nonlinear sigma model, we will demonstrate that it is possible to construct a renormalizable model without nonintegrable IR-UV mixing. Actually, we have the following.

(a) λ field propagator: $\Delta_\lambda(p) = -1/F_\lambda(p)$ where [see Fig. 2(a)]

$$F_\lambda(p) = N \int \frac{d^3k}{(2\pi)^3} \frac{1}{(k+p)^2 - m^2} \frac{1}{k^2 - m^2} \approx \frac{iN}{8\sqrt{-p^2}} \left(1 - \frac{4m}{\pi} \frac{1}{\sqrt{-p^2}} \right), \tag{22}$$

and the expression at the right corresponds to the large spacelike p behavior of $F_\lambda(p)$; as shown in the Appendix, for the analysis of the renormalization of the theory only the leading $1/\sqrt{-p^2}$ is relevant. It should be remarked also that the above propagator does not have poles and therefore does not have a particle content.

(b) Gauge field two-point proper function [Fig. 2(b)]:

$$F_{\mu\nu}(p) = N \int \frac{d^3k}{(2\pi)^3} \times \left\{ \frac{(2k+p)_\mu (2k+p)_\nu}{[(k+p)^2 - m^2](k^2 - m^2)} - \frac{2g_{\mu\nu}}{k^2 - m^2} \right\}, \tag{23}$$

which turns out to be finite if a gauge invariant regularization is adopted. Indeed, using dimensional regularization, we obtain

$$F_{\mu\nu}(p) = -\frac{iN}{8\pi} \left(g_{\mu\nu} - \frac{p_\mu p_\nu}{p^2} \right) p^2 F(p), \tag{24}$$

where

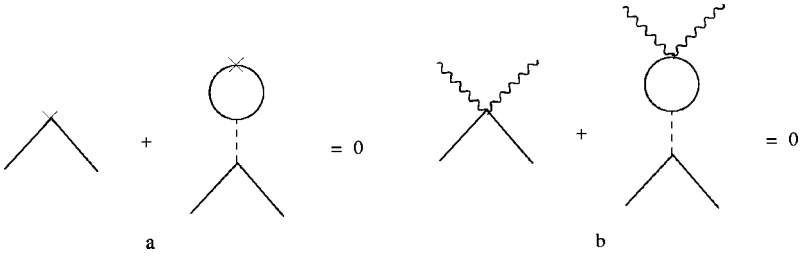

FIG. 3. Graphical identities for the CP^{N-1} model.

$$F(p)=\int_0^1 dx\,\frac{(1-2x)^2}{[m^2-p^2x(1-x)]^{1/2}}.$$

Differently from the λ field, the gauge field has a particle interpretation. Indeed, $F(0)=1/(3m)$ so that for small momenta A_μ behaves as a Maxwell field of intensity $\frac{1}{2}\sqrt{N/3\pi m}$ times the usual one. For large spacelike momenta

$$F_{\mu\nu}(p)\approx\frac{iN}{8\pi}\left(g_{\mu\nu}-\frac{p_\mu p_\nu}{p^2}\right)\left(\frac{\pi}{2}\sqrt{-p^2}-2m\right). \quad (25)$$

To get the propagator from Eq. (24) it is necessary to fix the gauge. We choose to work in the Landau gauge by adding to the Lagrangian (17) the term

$$-\frac{N}{2\alpha}(\partial_\mu A^\mu)*(\partial_\nu A^\nu)$$
$$+N\partial_\mu\bar{C}*[\partial^\mu C+i(C*A^\mu-A^\mu*C)] \quad (26)$$

and letting $\alpha\to 0$ after the calculation. Notice the presence of the Faddeev-Popov ghost term, which due to the non-Abelian character of the Moyal product does not decouple (the ghost fields will not show up in our leading order calculations but will be relevant in higher orders). It is now straightforward to verify that the gauge field propagator is given by

$$\Delta_{\mu\nu}(p)=-\frac{8\pi i}{N}\left(g_{\mu\nu}-\frac{p_\mu p_\nu}{p^2}\right)\frac{1}{p^2F(p)}$$
$$\approx\frac{16i}{N}\left(g_{\mu\nu}-\frac{p_\mu p_\nu}{p^2}\right)\left(\frac{1}{\sqrt{-p^2}}-\frac{4m}{\pi p^2}\right). \quad (27)$$

As a last remark, on the Feynman rules, note that, as in the commutative theory, any graph containing the diagrams of Fig. 2 as subgraphs must be omitted since those (sub)graphs were already considered (to construct the propagators for the A_μ and λ fields).

With these results at hand, we determine the ultraviolet degree of superficial divergence for a generic graph γ as being

$$d(\gamma)=3-N_A-2N_\lambda-\frac{N_\varphi}{2}-\frac{N_C}{2}, \quad (28)$$

where N_A, N_φ, N_λ, and N_C are the number of the external lines associated with the gauge, φ, λ, and ghost fields, respectively. Renormalization parts are those graphs having $d(\gamma)\geqslant 0$; in a noncommutative theory they occur only for planar (sub)graphs. Some of the ultraviolet divergences, associated with the planar graphs, may be absorbed by reparametrizations. As usual, we define the renormalized quantities by the replacements

$$A_\mu\to Z_A^{1/2}A_\mu=(1+a)A_\mu, \quad (29)$$

$$\varphi\to Z_\varphi^{1/2}\varphi=(1+b)^{1/2}\varphi, \quad (30)$$

$$\lambda\to Z_\lambda^{1/2}\lambda=(1+c)\lambda, \quad (31)$$

$$1/g\to Z_g/g=(1+d)/g, \quad (32)$$

so that the Lagrangian (17) written in terms of the new fields changes as $\mathcal{L}\to\mathcal{L}+\mathcal{L}_{ct}$, where the counterterm Lagrangian is given by

$$\mathcal{L}_{ct}=b\partial_\mu\varphi^\dagger*\partial^\mu\varphi-m^2b\varphi^\dagger\varphi$$
$$+iB(\partial_\mu\varphi^\dagger*A^\mu*\varphi-\varphi^\dagger*A^\mu*\partial_\mu\varphi)$$
$$+C\varphi^\dagger*A_\mu*A^\mu*\varphi+D\lambda*\varphi*\varphi^\dagger-FN\frac{\lambda}{g}, \quad (33)$$

where we introduced

$$B=(1+a)(1+b)-1, \quad (34)$$

$$C=(1+a)^2(1+b)-1, \quad (35)$$

$$D=(1+c)(1+b)-1, \quad (36)$$

$$F=(1+c)(1+d)-1. \quad (37)$$

These counterterms may be used to enforce m as the physical mass of the φ field, to ensure the elimination of the remaining divergences of the two-point function of the φ field and of the three-point function $\langle TA_\mu\varphi^\dagger\varphi\rangle$.

The analysis of the UV divergences is greatly facilitated with the aid of the graphical identities [11] depicted in Fig. 3. Due to the independence of the auxiliary field propagators on the noncommutative parameter, these identities are valid also in the present situation. It should be observed that, as the λ field has no particle content, the identities may be used even if we restrict ourselves to the one-particle irreducible graphs, i.e., to graphs that cannot be separated into disjoint pieces by cutting just one line, wavy or continuous. Before going any further we would like to stress some important consequences of these identities. As in the commutative case, the identity of Fig. 3(a) implies that the φ mass counterterm is innocuous since it cancels in all contributions to the Green functions.

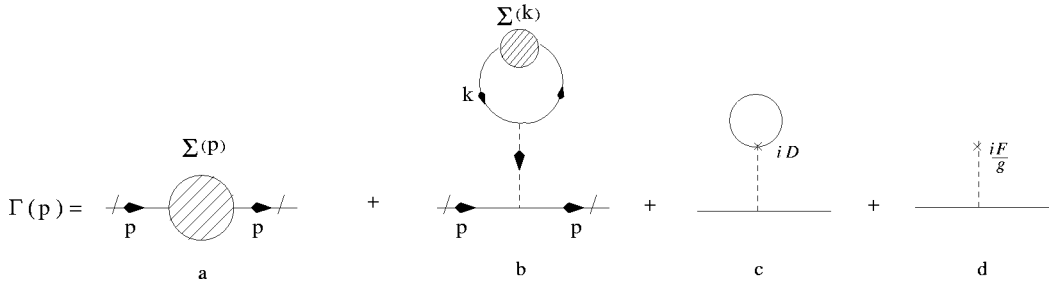

FIG. 4. Graphical structure of the φ field two-point function. The hatched bubble represents diagrams that are one-particle irreducible with respect to all fields.

This will be explicitly verified in our discussion of the renormalization of the two-point function of the φ field. Another implication of the graphical identity is that the $D\lambda\varphi^{\dagger}\varphi$ counterterm is also innocuous if we consider Green functions of the φ and A_{μ} fields only (no external λ lines); in that case D may be chosen at will and the wave function renormalization for the λ field is therefore irrelevant. In our approach the λ field tadpole contributions will not be considered separately but just in connection with the computation of the two-point Green function of the φ field.

An important implication of the identity of Fig. 3(b) is that, except for the second diagram of Fig. 2(b), all contributions containing the quadrilinear vertex will cancel pairwise; they need not be considered anymore. We also need to consider those divergences that do not have a corresponding counterterm. They may have N_{λ} equal to either 0 or 1. For $N_{\lambda}=1$, the dangerous divergences are associated with graphs with $N_{\varphi}=0$ and $N_A=1$. As mentioned earlier, this last possibility does not happen if a Lorentz covariant regularization is employed.

For $N_{\lambda}=0$ there are more possibilities:

(1) Graphs with $N_A=0$ and N_{φ} equal to either 4 or 6.
(2) Graphs with $N_A=1$ and $N_{\varphi}=4$.
(3) Graphs with $N_A=2$ and $N_{\varphi}=0$.
(4) Graphs with $N_A=3$ and $N_{\varphi}=0$.

Besides the UV behavior, in all cases we need to investigate the possible presence of infrared divergences (UV-IR mixing).

We focus first on the processes whose corresponding counterterms are correlated by gauge invariance, namely, corrections for the φ propagator, the three-point $\langle TA_{\mu}\varphi\varphi^{\dagger}\rangle$ and the four-point $\langle TA_{\mu}A^{\mu}\varphi^{\dagger}\varphi\rangle$ functions. We have the following:

(1) The subleading contributions to the self-energy of the φ field, $\Gamma(p)$, are shown in Figs. 4 and 5. They are purely planar and their (ultraviolet) divergences should be absorbed into a mass and wave function counterterms for the φ field. The mass counterterm is associated with the highest (quadratic) divergence gotten by setting to zero the external momentum of the contributing graphs. As can be easily checked, these divergences cancel between Figs. 4(a) and 4(b) due to the graphical identity of Fig. 3(a).

The contributions for the wave function renormalization of the φ field come from Figs. 5(a) and 5(b). Using dimensional regularization, a straightforward calculation furnishes the following results:

$$\Sigma_{\varphi}^{(a)}(p)=-i\int\frac{d^Dk}{(2\pi)^D}\frac{(k+2p)_{\mu}(k+2p)_{\nu}}{(k+p)^2-m^2}\Delta^{\mu\nu}(k)$$

$$=-i\frac{1}{N}\frac{64p^2}{3\pi^2\epsilon}+\text{finite terms}, \tag{38}$$

$$\Sigma_{\varphi}^{(b)}(p)=-i\int\frac{d^Dk}{(2\pi)^D}\frac{1}{(k+p)^2-m^2}\Delta_{\lambda}(k)$$

$$=C_b+i\frac{1}{N}\frac{4p^2}{3\pi^2\epsilon}+\text{finite terms}, \tag{39}$$

where $\epsilon=D-3$ and C_b is a quadratically divergent constant that would contribute to the mass renormalization of the φ field; as mentioned earlier, the mass renormalization terms cancel. Figure 5(c), on the other hand, cancels between Figs. 4(a) and 4(b) due to Fig. 3(b). The divergent parts are therefore eliminated by the counterterm $(1/N)(20/\pi^2\epsilon)\partial_{\mu}\varphi^{\dagger}\partial^{\mu}\varphi$, which fixes the divergent part of b as $b_{div}=(1/N)\times(20/\pi^2\epsilon)$. The overall divergences associated with the tadpole in Fig. 4(b) are absorbed in the counterterm in Fig. 4(d). We also assume that F possesses a finite part which enforces

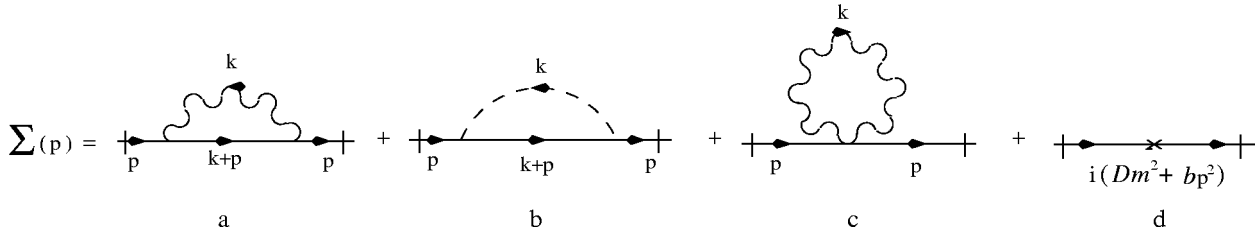

FIG. 5. Subleading contributions to the φ propagator.

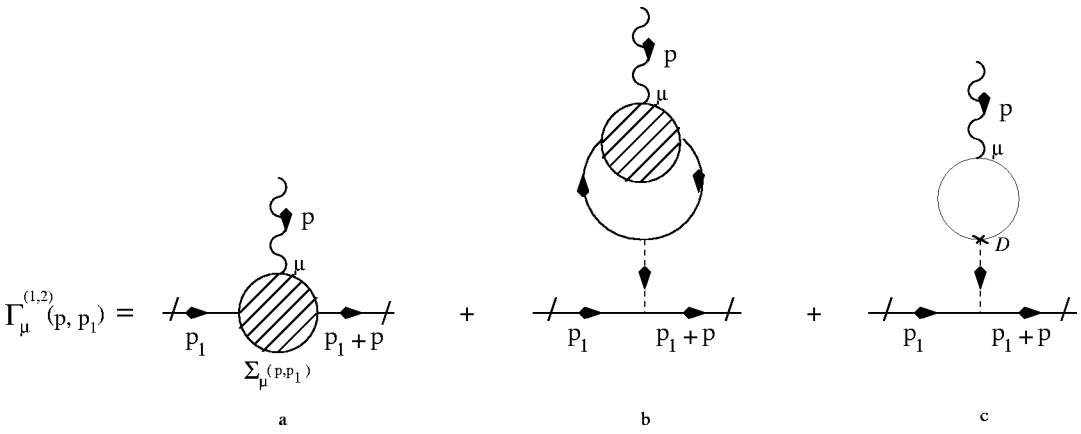

FIG. 6. General structure of the three-point vertex function of the A_μ and φ fields.

m as the physical mass, i.e., by adjusting F and b we impose the following normalization conditions:

$$\Gamma(p)=0 \quad \text{for } p^2=m^2, \tag{40}$$

$$\frac{\partial\Gamma}{\partial p^2}=0 \quad \text{for } p^2=m^2. \tag{41}$$

(2) Three-point function of the A_μ and φ fields, i.e., $\langle TA_\mu\varphi^\dagger\varphi\rangle$. Because of our previous remark on the cancellation of diagrams containing the quadrilinear vertex $A_\mu A^\mu\varphi^\dagger\varphi$, we have to analyze only those diagrams without this vertex, i.e., those which are depicted in Figs. 6 and 7. In Fig. 7 there are two one-loop diagrams and eight two-loop diagrams. Notice that the last four two-loop diagrams differ from the first four two-loop ones just by the orientation of the charge flow in the upper bosonic loop. In the commutative situation, graphs which differ just by the orientation of the charge flow are related by charge conjugation, and Furry's theorem states that they either give equal contributions or cancel between themselves. Here, however, charge conjugation is lost and Furry's theorem is no longer valid so that the contributions should be individually analyzed. In the construction of the diagrams implicit in Fig. 6(b) it is important to notice that any planar contribution is automatically overall ultraviolet finite. Indeed, these planar diagrams have zero degree of superficial divergence but, because of Lorentz covariance, they are proportional to p_μ, which lowers the effective degree of divergence by one unit. On the other hand, as we will show, the nonplanar contributions in Fig. 6(b) are used to cancel infrared divergences in the nonplanar diagrams of Fig. 7.

The first two diagrams shown in Fig. 7 are purely nonplanar and therefore are ultraviolet finite but could originate nonintegrable (linear) IR divergences. In fact, because of the transversality of the $\Delta_{\rho\sigma}$ propagator, Fig. 7(a) is finite and is given by

$$\int \frac{d^3k}{(2\pi)^3} e^{-i(2k\wedge p - p\wedge p_1)} \times \frac{[2(k+p_1)+p]_\mu [2(p_1+p)]_\rho 2p_{1\sigma}}{[(k+p_1)^2-m^2][(k+p_1+p)^2-m^2]} \Delta^{\rho\sigma}(k). \tag{42}$$

Due to the asymptotic behavior of $\Delta_{\rho\sigma}(k)$, this integral is finite even when the phase factor is absent so that the result is free from IR singularities. Figure 7(b), on the other hand, is linearly divergent at $p=0$. To see how this divergence is canceled we write its amplitude as

$$\int \frac{d^3k}{(2\pi)^3} e^{-i(2k\wedge p - p\wedge p_1)} I_\mu(k,p,p_1) = \int \frac{d^3k}{(2\pi)^3} e^{-i(2k\wedge p - p\wedge p_1)} [I_\mu(k,0,0) + R_\mu(k,p,p_1)], \tag{43}$$

where

$$I_\mu(k,p,p_1) = \frac{[2(k+p_1)+p]_\mu}{[(k+p_1)^2-m^2][(k+p_1+p)^2-m^2]} \Delta_\lambda(k) \tag{44}$$

and $R_\mu(k,p,p_1)$ presents at most logarithmic divergences. Explicitly,

$$\int \frac{d^3k}{(2\pi)^3} e^{-i(2k\wedge p - p\wedge p_1)} I_\mu(k,0,0) = \text{const} \times \frac{\tilde{p}_\mu}{\tilde{p}^2} e^{ip\wedge p_1}, \tag{45}$$

where we introduced a simplified notation $\tilde{p}^\mu = \Theta^{\mu\nu} p_\nu$. Now, among the diagrams implicit in Fig. 6(b) we consider the diagram of Fig. 8(a) which may be obtained from Fig.

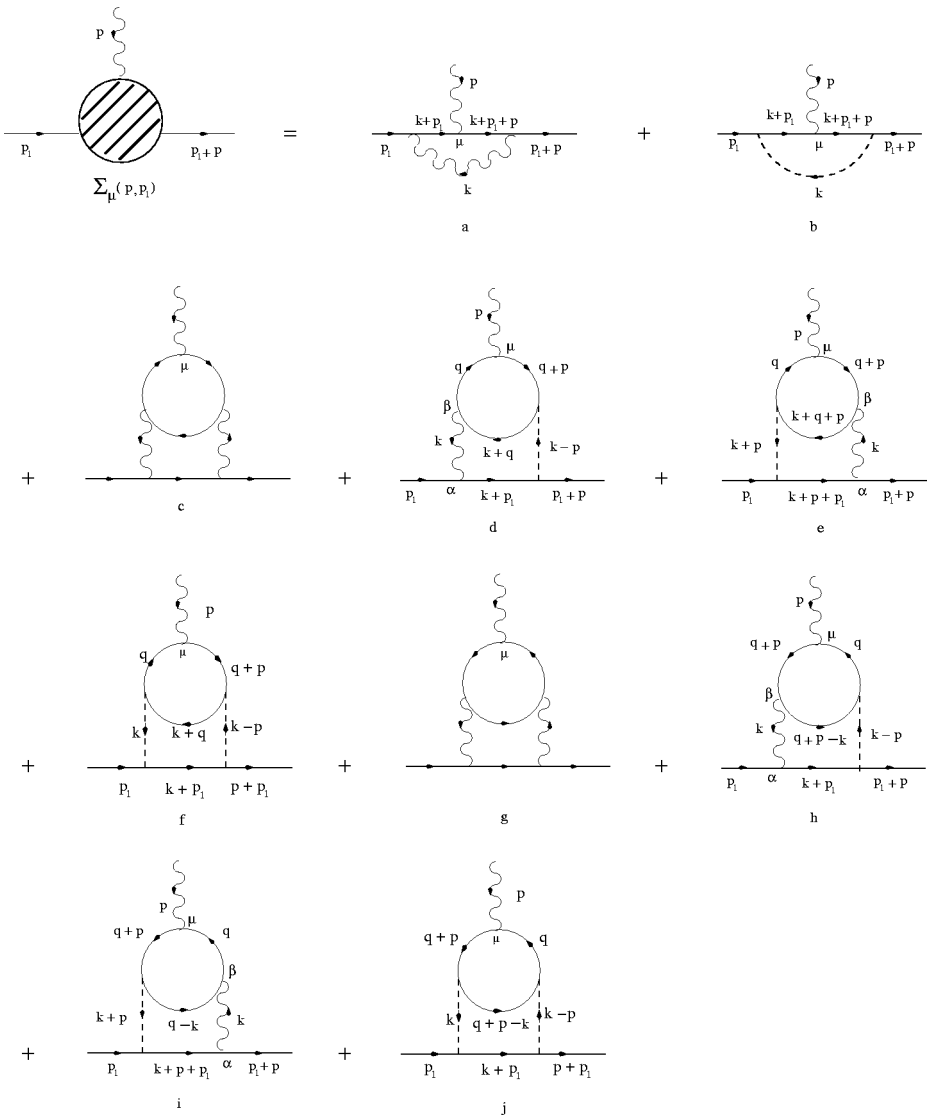

FIG. 7. Three-point function of the A_μ and φ fields.

7(b) by joining its φ external lines at a new $\lambda\varphi\varphi^\dagger$ vertex and attaching the external lines to a second $\lambda\varphi\varphi^\dagger$ vertex linked to the first one by the λ propagator. The amplitude for this graph reads

$$J_\mu(p,p_1)=\Delta_\lambda(p)\int \frac{d^3k}{(2\pi)^3}\frac{d^3q}{(2\pi)^3}e^{-i(2k\wedge p-p\wedge p_1)} \times I_\mu(k,p,q)\frac{i^2}{(q^2-m^2)[(q+p)^2-m^2]}. \tag{46}$$

Expanding $I_\mu(k,p,q)$ around $p=q=0$ as before and using Eq. (22) we get

$$J_\mu(p,p_1)=-\text{const}\times\frac{\tilde{p}_\mu}{\tilde{p}^2}e^{ip\wedge p_1} + \int \frac{d^3k}{(2\pi)^3}\frac{d^3q}{(2\pi)^3}e^{-i(2k\wedge p-p\wedge p_1)} \times R_\mu(k,p,q)\frac{i^2}{(q^2-m^2)[(q+p)^2-m^2]}\Delta_\lambda(p), \tag{47}$$

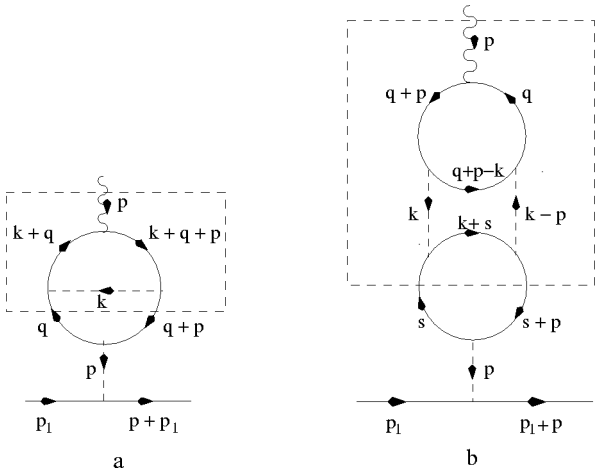

FIG. 8. Compensating diagrams for Figs. 7(b) and 7(j).

where the second term has at most logarithmic IR divergences. Thus, adding the two contributions, no dangerous IR divergence survives. This cancellation is just a manifestation of the identity expressed in Fig. 3(a). Being nonplanar, Figs. 7(a) and 7(b) do not present ultraviolet divergences either. This is an interesting point since in the renormalization of the commutative QED model the contribution of Fig. 7(a) is important to secure the gauge invariance of the perturbative method. The above procedure can be generalized for any linearly IR divergent graph. From any nonplanar graph γ we may construct a new diagram $\overline{\gamma}$ by joining two external φ lines of γ in a new trilinear vertex $\lambda\varphi\varphi^{\dagger}$. This new diagram contains γ as a subgraph so that it presents the same IR divergence as γ. The divergence in $\overline{\gamma}$ may be extracted by a simple Taylor expansion as we did in the above calculation. Summing the analytical expressions for γ and $\overline{\gamma}$ it remains only a mild logarithmic IR divergence.

The next set of graphs shown in Fig. 7 consists of four planar diagrams, Figs. 7(c)–7(f). As those graphs have two loops they may have one-loop divergent subgraphs. Here, however, we are concerned only with the overall divergence postponing the analysis of the divergences of the subgraphs to a later discussion (see Appendix). Figure 7(c) is actually finite since, due to the transversality of the gauge field propagator, the external vertices in the lower line cannot depend on the loop momentum containing the two wavy lines. In the following we list the divergent contributions arising from the Figs. 7(d)–7(f):

(a) Figure 7(d):

$$\Gamma^{(1,2)}_{\mu(d)} = -i4Ne^{-ip_1\wedge p}\int \frac{d^Dk}{(2\pi)^D}\frac{d^Dq}{(2\pi)^D}\frac{(2q+p)_\mu q_\beta p_{1\alpha}\Delta^{\alpha\beta}(k)\Delta_\lambda(k-p)}{[(k+p_1)^2-m^2][(k+q)^2-m^2](q^2-m^2)[(q+p)^2-m^2]}$$

$$= i(p_1)_\mu e^{-ip_1\wedge p}\frac{16}{3N\pi^2}\frac{1}{\epsilon} + \text{finite terms.} \tag{48}$$

(b) Figure 7(e):

$$\Gamma^{(1,2)}_{\mu(e)} = -iNe^{-ip_1\wedge p}\int \frac{d^Dk}{(2\pi)^D}\frac{d^Dq}{(2\pi)^D}\frac{(2q+p)_\mu(k+2q+2p)_\beta(k+2p+2p_1)_\alpha}{[(k+p+p_1)^2-m^2][(k+q+p)^2-m^2]}\frac{\Delta^{\alpha\beta}(k)\Delta_\lambda(k+p)}{(q^2-m^2)[(q+p)^2-m^2]}$$

$$= i(p_1+p)_\mu e^{-ip_1\wedge p}\frac{16}{3N\pi^2}\frac{1}{\epsilon} + \text{finite terms.} \tag{49}$$

(c) Figure 7(f):

$$\Gamma^{(1,2)}_{\mu(f)} = -iNe^{-ip_1\wedge p}\int \frac{d^Dk}{(2\pi)^D}\frac{d^Dq}{(2\pi)^D}\frac{(2q+p)_\mu\Delta_\lambda(k)\Delta_\lambda(k-p)}{[(k+p_1)^2-m^2][(k+q)^2-m^2]}\frac{1}{(q^2-m^2)[(q+p)^2-m^2]}$$

$$= -i(2p_1+p)_\mu e^{-ip_1\wedge p}\frac{2}{3N\pi^2}\frac{1}{\epsilon} + \text{finite terms.} \tag{50}$$

So altogether we have

$$\Gamma^{(1,2)}_{\mu(d)} + \Gamma^{(1,2)}_{\mu(e)} + \Gamma^{(1,2)}_{\mu(f)} = i(2p_1+p)_\mu e^{-ip_1\wedge p}\frac{14/3}{N\pi^2}\frac{1}{\epsilon} + \text{finite terms.} \tag{51}$$

The above divergence can be eliminated by the trilinear counterterm $(\frac{14}{3}i/N\pi^2\epsilon)A^\mu(\varphi\partial_\mu\varphi^{\dagger} - \partial_\mu\varphi\varphi^{\dagger})$, so that $B = \frac{14}{3}/N\pi^2\epsilon$.

Let us now consider the four nonplanar diagrams shown in Figs. 7(g)–7(j). As we have outlined in our discussion subsequent to Eq. (47), any infrared linear divergence can be eliminated by adequately combining the graphs. Nevertheless, in specific situations there are further additional simplifications. Indeed, we have the following:

(a) Figure 7(g): Because of our gauge choice, there is no IR divergence associated to that diagram.

(b) Figures 7(h) and 7(i): Again, due to our gauge choice these diagrams may present only a mild logarithmic IR divergence. This divergence is canceled by the corresponding diagrams implicit in Fig. 6(b).

(c) Figure 7(j): The amplitude associated with this diagram is linearly divergent at zero external momentum. Here

we apply the aforementioned construction which produces the graph shown in Fig. 8(b) [this is another graph implicit in Fig. 6(b)]. The leading IR divergences of these two diagrams cancels, as we proved earlier.

Our results can be used now to fix the value of C as defined in the counterterm Lagrangian (33). In fact, as $B=14/3N\pi^2\epsilon$, then $a=B-b_{div}=-46/3N\pi^2\epsilon$ so that $C=b_{div}+2a=-32/3N\pi^2\epsilon$. We remark that the only possible contributions of C would be for the next-to-leading corrections to the A_μ propagator; due to the graphical identity in Fig. 3(b) a nonvanishing C would have no effect up to the order we have been considering.

(3) Four-point function of the A^μ and φ fields, $\langle TA_\mu A_\nu \varphi^\dagger \varphi\rangle$. There are not ultraviolet divergences because a given graph is either nonplanar or one may find a "partner" graph to which the graphical identity in Fig. 3(a) may be applied. In the last case, the divergence in the original graph and its partner cancel pairwise. This is consistent with the fact that for this four-point function no counterterm is effective; in fact, the absence of these divergences may be considered as a test for the consistency of the calculation.

Although the renormalized Lagrangian turned out to be gauge invariant both in commutative and in the noncommutative cases, the mechanism by which this gauge invariance is achieved is entirely different in the two situations. Thus, Figs. 7(a) and 7(b), which are nonplanar, are ultraviolet finite, contrarily to the commutative case. On the other hand, in the noncommutative setting Furry's theorem is not valid and so many graph cancellations that hold in the commutative case are now absent and new contributions arise.

(4) Five-point function, $\langle TA_\mu \varphi^\dagger \varphi \varphi^\dagger \varphi\rangle$. The contributing diagrams are at most logarithmically divergent. In the planar part this divergence can be obtained by calculating the regularized amplitude at zero external momenta (after extracting the phase factors which in this case do not depend on the internal momentum). Because of Lorentz covariance, it is clear that the result of this computation vanishes so that no counterterm is needed. The possible IR divergence contained in the nonplanar diagrams of this type can be canceled using a construction similar to the one described after Eq. (47).

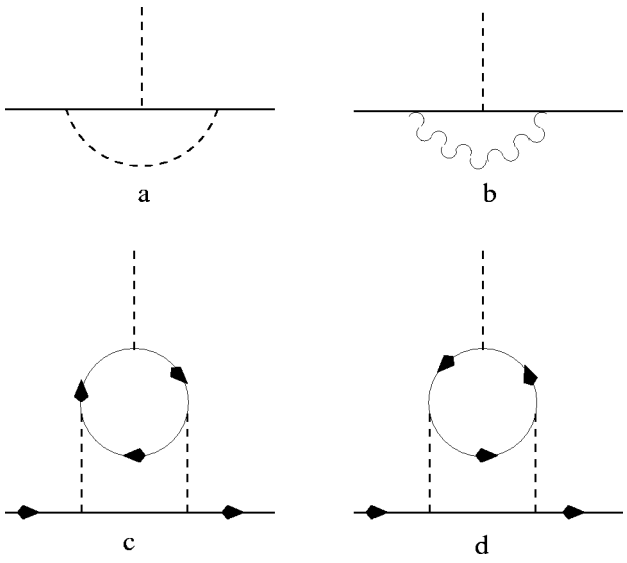

FIG. 9. Three-point function of the λ and φ fields.

(5) Three-point vertex function of the A_μ field, $\langle TA_\mu A_\nu A_\rho\rangle$. There are just two one-loop graphs that differ only by the orientation of the charge flow in the loop (each loop consists of three bosonic lines). These diagrams are both planar, and adding them together one gets a factor depending on the sine of the wedge product of the two external momenta times an integral which is finite by symmetric integration.

(6) Three-point vertex function of the λ and φ fields, $\langle T\lambda \varphi^\dagger \varphi\rangle$. To order $1/N$ the contributing graphs are depicted in Fig. 9. The one-loop graphs, Figs. 9(a) and 9(b), are nonplanar and therefore ultraviolet finite although in the infrared limit they may present a mild logarithmic divergence. The graph in Fig. 9(c), on the contrary, is planar and is ultraviolet logarithmically divergent. It has an analytic expression given by

$$\int \frac{d^3k}{(2\pi)^3}\frac{d^3q}{(2\pi)^3}\frac{e^{-i(p_1\wedge p)}}{[(k+p_1)^2-m^2][(k+p_1+p)^2-m^2][(k-q)^2-m^2]}\frac{1}{(q^2-m^2)}\Delta_\lambda(q+p_1)\Delta_\lambda(q+p_1+p). \quad (52)$$

Besides presenting an overall logarithmic divergence this integral has a divergent subintegral, namely, the q integration (this divergence will be examined in the context of the four-point function of the φ field, in the next item). The overall divergence cannot be eliminated through the use of the $D\lambda\varphi\varphi^\dagger$ counterterm since contributions containing such counterterms are canceled due to the identity of Fig. 3(a). However, as exemplified in the Appendix, the divergence mentioned is irrelevant as far the Green functions with only external φ and A_μ fields are concerned.

The analytic expression for Fig. 9(d) differs from Eq. (52) just by an additional factor $e^{-2iq\wedge p}$ and therefore is ultraviolet finite and has a mild logarithmic divergence when p tends to zero. Notice that in the commutative situation graphs Figs. 9(c) and 9(d) would give the same contributions, as a consequence of charge conjugation invariance. There are other graphs, not shown in Fig. 9, which differ from Figs. 9(c) and 9(d) just by the replacements, one at each time, of the internal dashed lines by wavy ones; because of the transversality of the A_μ propagator these additional graphs are ultraviolet

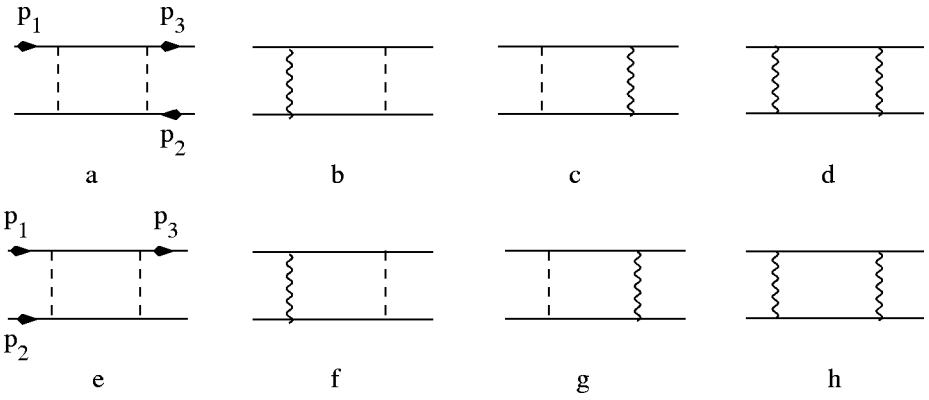

FIG. 10. Four-point function of the φ field.

finite and without infrared singularities.

(7) Concerning the contributions to the four-point function $\langle T\varphi\varphi\varphi^\dagger\varphi^\dagger\rangle$ let us first examine the one-loop diagrams. One sees that there are two types to be considered as they are depicted in Fig. 10. Whereas the graphs in the first row of Fig. 10 are ultraviolet linearly divergent, the graphs in the second row are nonplanar and therefore ultraviolet finites; they do not need counterterms. No counterterm is also needed for the four graphs of the first row because, as a consequence of the graphical identity of Fig. 3(a), there are two-loop graphs which cancel the mentioned divergences. For example, the highest (linear) divergence of the graph Fig. 10(a) is canceled by the one associated with the graph in Fig. 11(b). Figure 11(b) has a subgraph with the same divergence as Fig. 10(a). If we contract this subgraph to a point and use the identity of Fig. 3(a), we obtain the cancellation of these divergences. By a similar mechanism the logarithmic divergences which are proportional to the external momenta of the graph are also cancelled. The complete cancellation of all ultraviolet divergences can become complicate, as illustrated in the Appendix.

(8) Six-point function, $\langle T\varphi\varphi\varphi\varphi^\dagger\varphi^\dagger\varphi^\dagger\rangle$. As before, the divergences of the planar diagrams cancel pairwise by the use of the identity in Fig. 3(a), whereas the nonplanar graphs could at most develop a logarithmic infrared singularity.

The above discussion proves that, up to the leading nontrivial order of $1/N$, the noncommmutive CP^{N-1} model is renormalizable and without dangerous infrared singularities if the φ field transforms in accord with the left fundamental representation.

IV. THE NONCOMMUTATIVE CP^{N-1} MODEL IN THE ADJOINT REPRESENTATION

Let us now consider the leading $1/N$ contributions when the basic fields transform in accord with the adjoint representation. We will adopt the same graphical notation as in the previous section. However, we have new rules:

(1) Trilinear $A_\mu\varphi^\dagger\varphi$ vertex $\leftrightarrow -2(2k+p)_\mu \sin(k\wedge p)$.

(2) Quadrilinear $A^\mu A^\nu\varphi^\dagger\varphi$ vertex $\leftrightarrow -4ig^{\mu\nu}\sin(k_1\wedge p_1)\sin(k_2\wedge p_2)+p_1\leftrightarrow p_2$.

Note that these interactions are absent in the commutative limit.

Using these rules we fix the two-point function of the gauge field:

$$F_{\mu\nu}(p)=4N\Bigg[\int\frac{d^3k}{(2\pi)^3}\frac{(2k+p)_\mu(2k+p)_\nu}{(k^2-m^2)[(k+p)^2-m^2]}\sin^2(k\wedge p) - 2g_{\mu\nu}\int\frac{d^3k}{(2\pi)^3}\frac{1}{k^2-m^2}\sin^2(k\wedge p)\Bigg]. \tag{53}$$

As $\sin^2(k\wedge p)=\frac{1}{2}[1-\cos 2(k\wedge p)]$ we get a planar part that is twice that of the gauge field two-point function in the corresponding commutative theory. Concerning the nonplanar piece, we perform the standard procedures to obtain

$$F^{np}_{\mu\nu}(p)=-2N\int_0^1 dx\int\frac{d^3k}{(2\pi)^3}\frac{e^{ik\tilde{p}}}{[k^2-M^2]^2}\{4k_\mu k_\nu + p_\mu p_\nu(2x-1)^2-2g_{\mu\nu}[k^2+p^2(x-1)^2-m^2]\}, \tag{54}$$

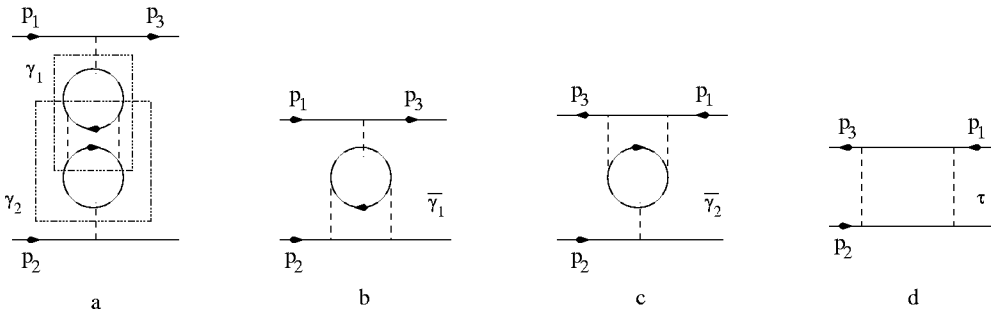

FIG. 11. Illustration of the mechanism for the complete cancellation of the UV divergences in the four-point function of the φ field. The first graph (G) contains γ_1, γ_2, and τ as subgraphs.

where $M^2=m^2-p^2x(1-x)$. Now, using Ref. [24],

$$\int \frac{d^3k}{(2\pi)^3}\frac{e^{ik_\alpha\tilde{p}^\alpha}}{[k^2-M^2]^2}=\frac{i}{(2\pi)^{3/2}\sqrt{4M}}\frac{K_{-1/2}[M\sqrt{-\tilde{p}^2}]}{(-\tilde{p}^2)^{-1/4}}=\frac{i}{8\pi}\frac{e^{-M\sqrt{-\tilde{p}^2}}}{M}, \tag{55}$$

where K_ν is the modified Bessel function of order ν, one obtains the complete two-point function of the gauge field (for simplicity we are employing the same notation used for the counterterms in the previous section; no confusion should arise since they refer to distinct situations)

$$F_{\mu\nu}(p)=(g_{\mu\nu}p^2-p_\mu p_\nu)A+\tilde{p}_\mu\tilde{p}_\nu B+p_\mu p_\nu C, \tag{56}$$

where

$$A=-\frac{Ni}{4\pi}\int_0^1 dx\left[\frac{1}{M}(1-2x)^2(1-e^{-M\sqrt{-\tilde{p}^2}})\right], \tag{57}$$

$$B=\frac{Ni}{\pi\tilde{p}^2}\int_0^1 dx\left(\frac{1}{\sqrt{-\tilde{p}^2}}+M\right)e^{-M\sqrt{-\tilde{p}^2}}, \tag{58}$$

and a gauge-fixing term was added. Note that this result possesses an infrared singularity at $\tilde{p}=0$.

Concerning the part of the Lagrangian which depends on the auxiliary field λ, we should recall that, as pointed out in Eq. (16), there is a two-parameter family of possible interaction terms; some simplifications occur depending on which form the interaction is chosen. In particular, note the following.

(1) If the interaction term containing λ is taken as in the preceding section, the computation of the two-point function of the λ field gives the same result as before but, differently from the left representation, the mixed propagator $\langle T\lambda A_\mu\rangle$ turns out to be nonvanishing. In fact, we find that at the leading order of $1/N$ the two-point function of the λ and A_μ fields is given by

$$\Gamma_{A_\mu\lambda}(p)=N\int\frac{d^3k}{(2\pi)^3}\frac{(2k+p)_\mu}{(k^2-m^2)[(k+p)^2-m^2]}e^{-i2k\wedge p}. \tag{59}$$

In contrast with the commutative model, the above expression does not vanish and yields

$$\Gamma_{A_\mu\lambda}(p)=-\frac{N\widetilde{p_\mu}}{4\pi\sqrt{-\tilde{p}^2}}\int_0^1 dx\, e^{-M\sqrt{-\tilde{p}^2}}\equiv D\tilde{p}_\mu, \tag{60}$$

where D is a nonvanishing function of $\tilde{p}^2$ and p^2.

(2) If the interaction term is chosen to be

$$\lambda*(\phi*\phi^\dagger-\phi^\dagger*\phi), \tag{61}$$

then, at the leading order of $1/N$, the mixed propagator vanishes but the λ field propagator will have a nonplanar contribution. In this case the two-point function of the λ field will be

$$2F_\lambda(p)+F_{np\lambda}(p)\equiv E(p), \tag{62}$$

where F_λ was given in Eq. (22) and the nonplanar part $F_{np\lambda}$ is

$$F_{np\lambda}(p)=-\frac{iN}{4\pi}\int_0^1 dx\frac{e^{-M\sqrt{-\tilde{p}^2}}}{M}. \tag{63}$$

As another consequence of the choice (61), the graphical identity of Fig. 3(a) is no longer valid. There are much more contributing diagrams than in the left representation.

We are now in a position which allows us to compute the propagators for the A_μ and λ fields at leading order of $1/N$. To encompass the two situations listed above, we shall designate the two-point function of the auxiliary λ field by $E(p)$ with the understanding that for case (1) $E(p)$ and $D(p)$ are given by Eqs. (22) and (60), respectively, whereas for case (2) $E(p)$ is given by Eq. (62) and $D(p)=0$. The propagators are then fixed by the inverse of the matrix which appears in the quadratic part of the Lagrangian. A direct calculation then furnishes the following.

For the A_μ propagator,

$$\Delta^{\mu\nu}=(g^{\mu\nu}p^2-p^\mu p^\nu)\frac{-1}{(p^2)^2A}+b\tilde{p}^\mu\tilde{p}^\nu-\frac{p^\mu p^\nu}{(p^2)^2C}, \tag{64}$$

where

$$b=\frac{-D^2}{[E(Ap^2+B\tilde{p}^2)-D^2\tilde{p}^2](Ap^2+B\tilde{p}^2)}+\frac{Bp^2}{p^2A(Ap^2+B\tilde{p}^2)}. \tag{65}$$

For the mixed propagator,

$$\Delta^\nu(p)\equiv\langle TA^\nu\lambda\rangle=d\tilde{p}^\nu, \tag{66}$$

where

$$d=\frac{D}{E(Ap^2+B\tilde{p}^2)-D^2\tilde{p}^2}. \tag{67}$$

For the λ propagator,

$$\Delta_\lambda(p)=-\frac{1}{E}(1+dD\tilde{p}^2). \tag{68}$$

At small momenta $b\simeq 1/p^2(-\tilde{p}^2)^{3/2}$ and $A\simeq\sqrt{-\tilde{p}^2}$ in both situations discriminated above and $d\simeq 1/\sqrt{-\tilde{p}^2}$ for case (1). Thus, the transversal part of the A_μ field propagator diverges badly [as $1/p^2(-\tilde{p}^2)^{1/2}$] at small momentum. In a local model such behavior would in a nonrelativistic limit be

associated with a potential that grows linearly with the distance from a charge probe. Therefore the quanta of the φ field would be confined. However, due to the nonlocal character of the interaction, there are at the vertices momentum-dependent form factors (sine factors) which smoothens the long-distance behavior of the potential.

Besides the aforementioned situation which indicates the possible occurrence of dangerous infrared singularities we would like to stress that, in fact, radiative corrections bring new infrared divergences that at higher order lead to the breakdown of the $1/N$ expansion. The crucial point of the calculation is provided by the corrections to the φ field two-point function whose contributions are again given by the graphs in Figs. 4 and 5 (we may have other diagrams containing the mixed propagator but these are nonplanar diagrams without IR or UV divergences). Let us first examine those contributions for the situation (1) listed above. Apart from Fig. 5(b) which is still planar, now there are trigonometric factors that deserve special consideration.

In the Landau gauge ($C\to\infty$), in which we have chosen to work, the transversality property of the gauge propagator produces a reduction of the degree of divergence of the graph in Fig. 5(a) by two units. Indeed the amplitude for Fig. 5(a) turns out to be

$$\int \frac{d^3k}{(2\pi)^3}\frac{(2p+k)_\mu(2p+k)_\nu}{(p+k)^2-m^2}\Delta^{\mu\nu}(k)\sin^2(k\wedge p) = 4p_\mu p_\nu\int \frac{d^3k}{(2\pi)^3}\frac{1}{(p+k)^2-m^2}\Delta^{\mu\nu}(k)\sin^2(k\wedge p). \tag{69}$$

The ultraviolet (logarithmic) divergence of this expression must be removed by an adequate counterterm; no infrared divergence appears because the sine factors improve the behavior of the integrand for small momenta. However, Fig. 5(c) has a leading contribution which, for high loop momenta, behaves as

$$\int \frac{d^3k}{(2\pi)^3}\cos(2k\wedge p)\frac{1}{\sqrt{k^2}} \tag{70}$$

and is quadratically divergent as p goes to zero. The multiple insertions of this graph into a larger graph leads to nonintegrable singularities which destroy the $1/N$ expansion. At this point we may wonder if this result could not be modified by another choice for the trilinear interaction among the λ and φ fields. In fact, the choice (61) as the interaction part involving the λ field introduces a sine factor at the trilinear vertex as it already happens with the $A_\mu A^\nu\varphi\varphi^\dagger$ vertex. If this is done, then diagram of Fig. 5(b) would have also a nonplanar part which asymptotically is similar to, Eq. (70). However, the numerical factors do not match and no cancellation could take place.

V. CONCLUDING REMARKS

In this work we focused on the construction of a consistent extension of the CP^{N-1} model to the noncommutative space. As we have seen, there are various possible extensions which depend on the way the fields transform under the gauge group. In all situations, we have chosen the auxiliary field λ as belonging to the adjoint representation. For the φ field belonging to the fundamental representation this prescription automatically prevents the appearance of a mixed $\langle T\lambda A_\mu\rangle$ propagator. In fact the possibility envisaged in Eq. (14) leads to a nonvanishing two-point proper function of the A_μ and λ fields given by

$$\Gamma_{A_\mu\lambda}(p) = -N\int \frac{d^3k}{(2\pi)^3}\frac{(2k+p)_\mu}{(k^2-m^2)[(k+p)^2-m^2]}e^{-i2k\wedge p} = \frac{iN\widetilde{p_\mu}}{8\pi\sqrt{-\tilde{p}^2}}\int_0^1 dx\, e^{-M\sqrt{-\tilde{p}^2}}. \tag{71}$$

For the φ field belonging to the adjoint representation, the mixing of the λ and A_μ fields will occur unless the constraint Lagrangian is used as in Eq. (61).

Up to the leading nontrivial order of $1/N$, all dangerous IR divergences were shown to cancel if the basic φ field belongs to the left representation of the gauge group. We also proved that the ultraviolet divergences may be absorbed into counterterms which preserve the form of the original Lagrangian. Therefore gauge invariance is maintained but this occurs in a way different from the commutative case. Indeed, in the commutative setting all the counterterms coefficients b, B, and C defined in Eq. (33) are equal and the A_μ field is not renormalized. In the present situation, however, the A_μ field gets renormalized and, although innocuous, a quadrilinear vertex $A_\mu A^\nu\varphi\varphi^\dagger$ counterterm occurs.

An entirely different picture is found if the basic field belongs to the adjoint representation. First, the graphical identities characteristics of the commutative model are no longer valid. Nonplanarity occurs already at the leading order of $1/N$ and the number of diagrams to be analyzed increases significantly. Also, due to the presence of (Moyal) commutators, the A_μ field formally decouples from the theory in the commutative limit. However, in this limit the Green functions are singular and the limit does not seem to exist (this is, of course, also true if the φ field is in the fundamental representation). Dangerous infrared divergences occur both in the gauge sector and in the radiative corrections to the two-point function of the φ field.

Because of the noncommutativity of the Moyal product there is a two-parameter family of interaction terms containing the auxiliary λ field. However, for no choice is it possible to cancel the divergences. Actually, the existence of IR-UV mixing suggests that to achieve consistency further extensions of the model should be investigated. This issue is the object of our next study where the inclusion of fermionic matter fields will be investigated.

ACKNOWLEDGMENTS

This work was partially supported by Fundação de Amparo à Pesquisa do Estado de São Paulo (FAPESP) and Conselho Nacional de Desenvolvimento Científico e Tecnológico (CNPq).

APPENDIX

In this appendix we shall demonstrate some results concerning the ultraviolet behavior of the noncommutative CP^{N-1} model when the basic φ field belongs to the left fundamental representation of the gauge group. They are as follows.

(a) The subleading contributions to the λ and A_μ propagators, which are explicit in Eqs. (22) and (25), are irrelevant as far as the ultraviolet divergences are concerned. In fact, the only case that requires special attention is the two-point function of the φ field, which becomes at most linearly divergent if the subleading contribution for the auxiliary fields is used. Actually, it only occurs in the diagram of Fig. 5(b) up to the order that we have considered. Replacing this contribution in Figs. 4 and 5 one sees that the would-be linear divergences cancel among themselves. The next subdivergence which is only logarithmic vanishes due to Lorentz covariance.

(b) Contributions containing the mass counterterm cancel pairwise. This result follows straightforwardly from the graphical identity depicted in Fig. 3(a) where the special vertex stands for the mass counterterm insertion.

(c) Finally we will exemplify how the complete cancellation of ultraviolet divergences takes place in the case where several (sub)diagrams are involved, as in the three-loop diagram G of Fig. 11. The ultraviolet divergent subgraphs of G are $\gamma_1, \gamma_2,$ and τ; they also occur as (sub)graphs of the diagrams $\overline{\gamma_1}, \overline{\gamma_2}$, and τ as shown in Fig. 11 (in spite of having a different number of loops they are of the same order in $1/N$). These diagrams are all planar and have the same noncommutative phase ($\exp i[p_1 \wedge p_2 - p_1 \wedge p_3 + p_2 \wedge p_3]$) which therefore factorizes in their sum. Notice that γ_1 and γ_2 are overlapping and that both contain τ as a subgraph. In the Bogolubov-Parasiuk-Hepp-Zimmermann (BPHZ) scheme the relevant G forests are $\emptyset, \gamma_1, \gamma_2, \tau, \{\gamma_1, \tau\}$ and $\{\gamma_2, \tau\}$. The BPHZ-subtracted amplitude associated with graph G is therefore

$$R_G = I_G - I_{G/\gamma_1} t^0_{\gamma_1} I_{\gamma_1} - I_{G/\gamma_2} t^0_{\gamma_2} I_{\gamma_2} - I_{G/\tau} t^1_\tau I_\tau + I_{G/\gamma_1} t^0_{\gamma_1} I_{\gamma_1/\tau} t^1_\tau I_\tau + I_{G/\gamma_2} t^0_{\gamma_2} I_{\gamma_2/\tau} t^1_\tau I_\tau, \quad \text{(A1)}$$

where I_G denotes the unsubtracted amplitude associated with graph G; as usual, $I_{G/\gamma}$ is the amplitude associated to the reduced graph G/γ obtained by contracting the subgraph γ of G to a point. For a generic diagram γ, t_γ is defined as the Taylor operator on the external independent momenta of γ with the proviso that it does not act on the noncommutative phase factor. Similarly, the BPHZ-subtracted amplitudes for the graphs $\overline{\gamma_1}$, $\overline{\gamma_2}$, and τ are

$$R^-_{\gamma_1} = I^-_{\gamma_1} - I^-_{\gamma_1/\gamma_1} t^0_{\gamma_1} I_{\gamma_1} - I^-_{\gamma_1/\tau} t^1_\tau I_\tau + I^-_{\gamma_1/\gamma_1} t^0_{\gamma_1} I_{\gamma_1/\tau} t^1_\tau I_\tau, \quad \text{(A2)}$$

$$R^-_{\gamma_2} = I^-_{\gamma_2} - I^-_{\gamma_2/\gamma_2} t^0_{\gamma_2} I_{\gamma_2} - I^-_{\gamma_2/\tau} t^1_\tau I_\tau + I^-_{\gamma_2/\gamma_2} t^0_{\gamma_2} I_{\gamma_2/\tau} t^1_\tau I_\tau, \quad \text{(A3)}$$

and

$$R_\tau = I_\tau - t^1_\tau I_\tau. \quad \text{(A4)}$$

Note now that as a consequence of the graphical identity in Fig. 3(a), $I_{G/\gamma_1} = I_{G/\gamma_2} = -I^-_{\gamma_1/\gamma_1} = -I^-_{\gamma_2/\gamma_2}$ and that $I_{G/\tau} = -I^-_{\gamma_1/\tau} = -I^-_{\gamma_2/\tau} =$ trivial four vertex, we see that when adding the above contributions all the subtraction terms cancel. We stress that the cancellation occurs for all subtractions including those associated with the last subtraction for the linearly divergent diagram τ (in this case, to the reduced vertex associated to the contraction of τ to a point it is assigned a linear polynomial in the external momenta of τ). This proves that the sum of the unsubtracted diagrams is finite.

If the charge flow in the upper and lower loops of Fig. 11 are in opposite direction, the corresponding diagrams are nonplanar. They still have the same phase factor but it depends on the loop momentum of the τ diagram. Individually they present a linear infrared divergence which nonetheless is cancelled whenever they are added. This is most easily seen by factorizing the noncommutative phases and then Taylor expanding the remaining of the τ's integrand up to first order in the independent external momenta of that graph.

[1] N.A. Nekrasov and M. Douglas, Rev. Mod. Phys. **73**, 977 (2002); R.J. Szabo, Phys. Rep. **378**, 207 (2003); M. Gomes, in *Proceedings of the XI Jorge André Swieca Summer School, Particles and Fields*, edited by G.A. Alves, O.J.P. Éboli, and V.O. Rivelles (World Scientific, Singapore, 2002); H.O. Girotti, "Noncommutative Quantum Field Theories," hep-th/0301237.

[2] S. Minwalla, Van Raamsdonk, and N. Seiberg, J. High Energy Phys. **02**, 020 (2000).

[3] L. Griguolo and M. Pietroni, J. High Energy Phys. **05**, 032 (2001).

[4] A.A. Bichl, J.M. Grimstrup, H. Grosse, L. Popp, M. Schweda, and R. Wulkenhaar, J. High Energy Phys. **10**, 046 (2000).

[5] H.O. Girotti, M. Gomes, V.O. Rivelles, and A.J. da Silva, Nucl. Phys. **B587**, 299 (2000).

[6] H.O. Girotti, M. Gomes, A.Yu. Petrov, V.O. Rivelles, and A.J. da Silva, Phys. Lett. B **521**, 119 (2001); H.O. Girotti, M. Gomes, V.O. Rivelles, and A.J. da Silva, Int. J. Mod. Phys. A **17**, 1503 (2002).

[7] A. Matusis, L. Susskind, and N. Toumbas, J. High Energy Phys. **12**, 002 (2000).

[8] D. Zanon, Phys. Lett. B **504**, 101 (2001); M. Pernici, A. San-

tambrogio, and D. Zanon, *ibid.* **504**, 131 (2001); A. Santambrogio and D. Zanon, J. High Energy Phys. **01**, 024 (2001).

[9] J. Polchinski, Nucl. Phys. **B231**, 269 (1984); M. Bonini, M. D'Attanasio, and G. Marchesini, *ibid.* **B409**, 441 (1993).

[10] A. D'Adda, M. Lüscher, and P. di Vecchia, Nucl. Phys. **B146**, 63 (1978); A. D'Adda, P. di Vecchia, and M. Lüscher, *ibid.* **B152**, 125 (1979).

[11] Ya. Aref'eva, Ann. Phys. (N.Y.) **117**, 393 (1979); Ya. Aref'eva and S.I. Azakov, Nucl. Phys. **B162**, 298 (1980).

[12] R. Köberle and V. Kurak, Phys. Rev. Lett. **58**, 627 (1987); Phys. Rev. D **36**, 627 (1987); E. Abdalla, M.C.B. Abdalla, and M. Gomes, *ibid.* **27**, 825 (1983); E. Abdalla, M. Forger, and M. Gomes, Nucl. Phys. **B210**, 181 (1982); B. Berg, M. Karowski, V. Kurak, and P. Weisz, *ibid.* **B134**, 125 (1978).

[13] S.H. Park, Phys. Rev. D **45**, 3332 (1992).

[14] D.K. Hong and J.Y. Kim, Phys. Lett. B **383**, 327 (1996).

[15] G. Ferretti and S.G. Rajeev, Mod. Phys. Lett. A **7**, 2087 (1992).

[16] M.M. Sheikh-Jabbari, Phys. Rev. Lett. **84**, 5265 (2000); M. Chaichian, K. Nishijima, and A. Tureanu, Phys. Lett. B **568**, 146 (2003).

[17] Logarithmic infrared divergences resulting from the IR-UV mixing may occur but these are not dangerous because they are integrable. As discussed in Ref. [2], unlike the case of logarithmic divergences, multiple insertions of quadratic or linear infrared divergent graphs into a larger graph will produce nonintegrable singularities.

[18] M. Hayakawa, Phys. Lett. B **478**, 394 (2000).

[19] H. Weyl, Z. Phys. **46**, 1 (1949).

[20] J.E. Moyal, Proc. Cambridge Philos. Soc. **45**, 99 (1949).

[21] T. Filk, Phys. Lett. B **376**, 53 (1996).

[22] J. Gomis and T. Mehen, Nucl. Phys. **B591**, 265 (2000); L. Alvarez-Gaume, J.L.F. Barbon, and R. Zwicky, J. High Energy Phys. **05**, 057 (2001); A. Bassetto, L. Griguolo, G. Nardelli, and F. Vian, *ibid.* **07**, 008 (2001); Yi Liao and K. Sibold, Eur. Phys. J. C **25**, 479 (2002); D. Bahns, S. Doplicher, K. Fredenhagen, and G. Piacitelli, Phys. Lett. B **533**, 178 (2002).

[23] M. Chaichian, C. Montonen, and A. Tureanu, Phys. Lett. B **566**, 263 (2003); M. Chaichian, M.N. Mnatsakanova, A. Tureanu, and Yu.S. Vernov, Nucl. Phys. **B673**, 476 (2003); T. Ohl, R. Rueckl, and J. Zeiner, *ibid.* **B676**, 229 (2004).

[24] I. M. Gel'fand and G. E. Shilov, *Generalized Functions* (Academic, New York, 1964), Vol. 1.